Electromagnetic fields and the radiation of a charged particle rotating along a closed trajectory around a dielectric cylinder

A S Kotanjyan and A A Saharian

Yerevan State University, 1 Alex Manoogian Street, 0025 Yerevan, Armenia
Institute of Applied Problems in Physics, 25 Nersessian Street, 0014 Yerevan, Armenia

E-mail: anna.kotanjyan@ysu.am, saharian@ysu.am

Abstract. We investigate the electromagnetic fields and the radiation intensity for a charged particle moving along an arbitrary closed orbit around a dielectric cylinder immersed into a homogeneous medium. These results generalize our previous research in the special case of a circular orbit. For the latter geometry it has been shown that under certain conditions strong narrow peaks appear in the angular distribution of the radiation intensity in the exterior medium. We discuss the influence of the trajectory shift from the circular one on the characteristics of the peaks.

1. Introduction

Due to the unique characteristics of synchrotron radiation, such as broad spectrum, high flux, high brilliance, it has wide applications (for reviews see [1]-[3]). Synchrotron light is an ideal tool for many types of research and also has industrial applications including materials science, biological and life sciences, medicine, chemistry. The wide applications of the synchrotron radiation motivate the importance of investigations for various mechanisms of control for the radiation parameters. In particular, it is of interest to consider the influence of a medium on the characteristics of the radiation. The synchrotron radiation from a charged particle circulating in a homogeneous medium was considered in [4]-[9], where it has been shown that the interference between the synchrotron and Cherenkov radiations leads to remarkable effects. New interesting features arise in the case of inhomogeneous media.

In a series of papers [10]-[16], we have investigated the influence of cylindrical boundaries between two dielectrics on the characteristics of the synchrotron radiation. It has been shown that under the Cherenkov condition for the material of the cylinder and the particle velocity, strong narrow peaks appear in the angular distribution of the radiation intensity in the exterior medium with respect to the dielectric cylinder. At these peaks the radiated energy exceeds the corresponding quantity in the case of a homogeneous medium by several orders of magnitude. The radiation propagating inside the dielectric cylinder is studied in [17, 18]. Similar features for the radiation generated by a charge moving along a helical orbit around/inside a dielectric cylinder have been investigated in [19]-[22]. The corresponding problem for a charge moving in vacuum has been widely discussed in the literature (see, for instance, [2, 3] and references given therein).

In the previous research we have assumed that the particle moves along a circular trajectory concentric with the cylinder axis or, in the case of helical motion, the projection of the helix on the plane perpendicular to the cylinder axis is a concentric circle. In realistic situations the trajectory of the particle may differ from the concentric circular one and it is of interest to investigate the influence of this shift on the parameters of the peaks in the radiation intensity. In the present paper we consider the electromagnetic fields and the radiation intensity from a charge moving around a dielectric cylinder along a trajectory the projection of which on the plane perpendicular to the cylinder axis is an arbitrary closed curve.

2. Electromagnetic fields in the exterior medium

Consider a point charge q moving along a helical trajectory around a dielectric cylinder with radius ρ_c. The permittivity for the cylinder will be denoted by ε_0 and the cylinder is immersed in a homogeneous medium with dielectric permittivity ε_1 (magnetic permeabilities will be taken to be unit). In what follows the cylindrical coordinate system (ρ, ϕ, z), with the axis z directed along the cylinder axis, will be used. We will assume that the projection of the particle trajectory on the plane perpendicular to the z-axis is an arbitrary closed curve and the corresponding motion of the charge is described by the functions $\rho = \rho_e(t)$ and $\phi = \phi_e(t)$ with $\rho_e(t) > \rho_c$. The latter condition means that the charge does not cross the cylinder surface. The projection of the charge velocity along the z-axis will be denoted $v_\parallel$ assuming that it is a constant. The components of the current density created by charge are given by the formula

$$j_l = (v_l q/\rho)\delta(\rho - \rho_e(t))\delta(\phi - \phi_e(t))\delta(z - v_\parallel t), \ l = \rho, \phi, z, \tag{1}$$

where v_ρ and v_ϕ are the corresponding components of the charge velocity.

By making use of the formula for the Green function given earlier in [10], in the Lorentz gauge for the vector potential one finds the following expression (the details will be presented elsewhere)

$$A_l(\mathbf{r},t) = -\frac{q}{\pi c} \sum_{m,n=-\infty}^{+\infty} \sum_{l'=\rho,\phi,z} \int_{-\infty}^{+\infty} dk_z \, G_{ll',n}(m, k_z, \omega_n(k_z), \rho) e^{im\phi + ik_z z - i\omega_n(k_z)t}, \tag{2}$$

where

$$\omega_n(k_z) \equiv n\omega_0 + k_z v_\parallel, \ \omega_0 = 2\pi/T, \tag{3}$$

with T being the period of the transverse motion. For the functions in the integrand of (2) we have

$$G_{ll',n}(m, k_z, \omega, \rho) = \frac{\pi}{4i^{\sigma_l + 1 - \sigma_{l'}}} \sum_{p=\pm 1} p^{\sigma_l - \sigma_{l'}} B_{l',m,n}^{(p)} H_{m+p}(\lambda_1 \rho),$$

$$G_{lz,n}(m, k_z, \omega, \rho) = \frac{i^{2-\sigma_l} k_z}{2\rho_c} H_{m,m,z}(n, \lambda_1) \frac{J_m(\lambda_0 \rho_c)}{\alpha_m V_m^H} \sum_{p=\pm 1} p^{\sigma_l - 1} \frac{J_{m+p}(\lambda_0 \rho_c)}{V_{m+p}^H} H_{m+p}(\lambda_1 \rho), \tag{4}$$

$$G_{zz,n}(m, k_z, \omega, \rho) = -(i\pi/2)\left[J_{m,m,z}(n, \lambda_1) - H_{m,m,z}(n, \lambda_1) V_m^J / V_m^H\right] H_m(\lambda_1 \rho),$$

where $l, l' = \rho, \phi$, $\sigma_\rho = -\sigma_\phi = 1$ and $G_{z\rho,n}(m, k_z, \omega, \rho) = G_{z\phi,n}(m, k_z, \omega, \rho) = 0$. In (4), $J_m(x)$ is the Bessel function, $H_m(x) \equiv H_m^{(1)}(x)$ is the Hankel function of the first kind. We have also defined new functions

$$F_{m',m,l}(n, \lambda_1) = \frac{1}{T} \int_0^T dt \, v_l(t) F_{m'}(\lambda_1 \rho_e(t)) e^{-im\phi_e(t) + in\omega_0 t}, \ F = J, H, \tag{5}$$

with $\lambda_j^2 = \omega_n^2(k_z)\varepsilon_j/c^2 - k_z^2$, $j = 0, 1$. Other notations used in (4) are as follows:

$$V_m^F = J_m(\lambda_0\rho_c)\frac{\partial F_m(\lambda_1\rho_c)}{\partial\rho_c} - F_m(\lambda_1\rho_c)\frac{\partial J_m(\lambda_0\rho_c)}{\partial\rho_c}, \ F = J, H, \tag{6}$$

and

$$\begin{aligned} B_{l,m,n}^{(p)} &= J_{m+p,m,l}\left(n, \lambda_1\right) - H_{m+p,m,l}\left(n, \lambda_1\right)V_{m+p}^J/V_{m+p}^H \\ &+ \frac{ip^{\sigma_l-1}\lambda_0}{\pi\rho_c\alpha_m}J_m(\lambda_0\rho_c)\frac{J_{m+p}(\lambda_0\rho_c)}{V_{m+p}^H}\sum_{p'=\pm1}p'^{\sigma_l}\frac{H_{m+p',m,l}\left(n, \lambda_1\right)}{V_{m+p'}^H}. \end{aligned} \tag{7}$$

The function α_m is defined by the relation

$$\alpha_m = \frac{\varepsilon_0}{\varepsilon_1 - \varepsilon_0} - \frac{\lambda_0 J_m(\lambda_0\rho_c)}{2}\sum_{p=\pm1}p\frac{H_{m+p}(\lambda_1\rho_c)}{V_{m+p}^H}. \tag{8}$$

Note that the equation $\alpha_m = 0$ determines the eigenmodes of the dielectric cylinder.

With the vector potential (2) we can find the electric and magnetic fields by using the standard formulas. In the special case of circular helix coaxial with the cylinder axis one has $F_{m',m,l}\left(n, \lambda_1\right) = v_l F_{m'}(\lambda_1\rho_e)\delta_{nm}$ and the expressions given above are reduced to the ones derived in [22].

3. Radiation intensity

Having the electromagnetic fields we can investigate the intensity of the radiation propagating in the exterior medium. For $\lambda_1^2 < 0$ the corresponding Fourier components are exponentially damped for large values ρ, and the radiation at large distances from the cylinder is present only under the condition $\lambda_1^2 > 0$. The average energy flux per unit time through the cylindrical surface of radius ρ, coaxial with the dielectric cylinder, is given by the Poynting vector:

$$I = \frac{c}{4\pi T}\int_0^T dt\int_0^{2\pi}d\phi\int_{-\infty}^{+\infty}dz\,\rho\mathbf{n}_\rho\cdot[\mathbf{E}\times\mathbf{H}]. \tag{9}$$

At large distances from the cylinder, the variable k_z in the formulas given above corresponds to the projection of the wave vector for the radiated photon on the z-axis. Instead of k_z it is convenient to introduce the angle θ between the photon wave vector and the cylinder axis in accordance with the relation

$$k_z = \frac{n\omega_0}{c}\frac{\sqrt{\varepsilon_1}\cos\theta}{1 - \beta_{1\parallel}\cos\theta}, \ \beta_{1\parallel} = \frac{v_\parallel}{c}\sqrt{\varepsilon_1}. \tag{10}$$

For the radiation frequency one has $|\omega_n|$ with

$$\omega_n = n\omega_0/(1 - \beta_{1\parallel}\cos\theta). \tag{11}$$

Hence, n determines the harmonic number of the radiation. We also have the following expressions for λ_1 and λ_0:

$$\lambda_1 = \frac{n\omega_0}{c}\frac{\sqrt{\varepsilon_1}\sin\theta}{1 - \beta_{1\parallel}\cos\theta}, \quad \lambda_0 = \frac{n\omega_0}{c}\frac{\sqrt{\varepsilon_0 - \varepsilon_1\cos^2\theta}}{1 - \beta_{1\parallel}\cos\theta}. \tag{12}$$

The angular density of the radiation intensity at a given harmonic n, $dI_n/d\Omega$, with $d\Omega = \sin\theta d\theta d\phi$ being the solid angle element, is defined by

$$I = \sum_{n=-\infty}^{+\infty} \int d\Omega \frac{dI_n}{d\Omega}. \tag{13}$$

By using (2), at large distances from the cylinder, for the angular distribution of the radiated energy per unit time we find

$$\frac{dI_n}{d\Omega} = \frac{q^2}{4\pi^3 c} \frac{n^2 \omega_0^2 \sqrt{\varepsilon_1}}{\left|1 - \beta_{1\parallel}\cos\theta\right|^3} \sum_{m=-\infty}^{+\infty} \left[\left| \sum_{p=\pm 1} p D_{m,n}^{(p)} \right|^2 + \left| \sum_{p=\pm 1} D_{m,n}^{(p)} \right|^2 \cos^2\theta \right], \tag{14}$$

with the notation

$$
\begin{aligned}
D_{m,n}^{(p)} &= \frac{\pi}{2ic} \left[J_{m+p,m}(n,\lambda_1) - H_{m+p,m}(n,\lambda_1) \frac{V_{m+p}^J}{V_{m+p}^H} \right] \\
&+ \frac{i\pi\lambda_1}{2ck_z} \left[J_{m,m,z}(n,\lambda_1) - H_{m,m,z}(n,\lambda_1) \frac{V_m^J}{V_m^H} \right] \\
&+ p \frac{J_m(\lambda_0 \rho_c)}{c\rho_c \alpha_m} \frac{J_{m+p}(\lambda_0 \rho_c)}{V_{m+p}^H} \left[\frac{k_z}{V_m^H} H_{m,m,z}(n,\lambda_1) + \frac{\lambda_0}{2} \sum_{l=\pm 1} \frac{H_{m+l,m}(n,\lambda_1)}{V_{m+l}^H} \right], \quad (15)
\end{aligned}
$$

and

$$F_{m+p,m}(n,\lambda_1) = F_{m+p,m,\phi}(n,\lambda_1) - ip F_{m+p,m,\rho}(n,\lambda_1), \ F = J, H. \tag{16}$$

First let us consider a special case of a circular helix with $\rho_e(t) = \rho_e = \text{const}$ and $\phi_e(t) = \omega_0 t$. In this case $v_\rho = 0$ and $F_{m',m,l}(n,\lambda_1) = v_l F_{m'}(\lambda_1 \rho_e)\delta_{nm}$. Hence, in (14) the term $m = n$ contributes only. The features of the radiation intensity in this special case have been discussed in [22]. By using Debye's asymptotic expansions for the Bessel and Neumann functions, it can be seen that under the condition $|\lambda_1|\rho_c < n$, at points where the real part of the function α_n, given by formula (8), is equal to zero, the contribution of the imaginary part of this function into the coefficients $D_{n,n}^{(p)}$ can be exponentially large for large values n. This leads to the appearance of strong narrow peaks in the angular distribution for the radiation intensity at a given harmonic n. The condition for the real part of the function α_n to be zero has the form:

$$\sum_{l=\pm 1} \left[\frac{\lambda_1}{\lambda_0} \frac{J_{n+l}(\lambda_0 \rho_c) Y_n(\lambda_1 \rho_c)}{J_n(\lambda_0 \rho_c) Y_{n+l}(\lambda_1 \rho_c)} - 1 \right]^{-1} = \frac{2\varepsilon_0}{\varepsilon_1 - \varepsilon_0}, \tag{17}$$

where $Y_\nu(x)$ is the Neumann function. Note that (17) is obtained from the equation determining the eigenmodes for the dielectric cylinder by the replacement $H_n \to Y_n$. Equation (17) has no solutions for $\lambda_0^2 < 0$, which is possible only for $\varepsilon_0 < \varepsilon_1$. Hence, the peaks do not appear for the case $\lambda_0^2 < 0$ which corresponds to the angular region $\cos^2\theta > \varepsilon_0/\varepsilon_1$. As necessary conditions for the presence of the strong narrow peaks in the angular distribution for the radiation intensity one has

$$\varepsilon_0 > \varepsilon_1, \ \tilde{v}\sqrt{\varepsilon_0}/c > 1, \tag{18}$$

where $\tilde{v} = \sqrt{v_\parallel^2 + \omega_0^2 \rho_c^2}$ is the velocity of the charge image on the cylinder surface. The second condition in (18) is the Cherenkov condition for the velocity of the charge image on the cylinder

surface and dielectric permittivity of the cylinder. In figure 1, the full curve displays the dependence of the angular density for the number of the quanta radiated per unit time,

$$\frac{dN_n}{d\Omega} = \frac{1}{\hbar|\omega_n|}\frac{dI_n}{d\Omega}, \tag{19}$$

as a function of the angle θ for the parameters $\beta_{1\perp} = 0.9$, $\beta_{1\parallel} = 0.4$, $\rho_c/\rho_e = 0.95$, $n = 10$. We assumed that the cylinder is made of fused quartz with permittivity $\varepsilon_0 = 3.75$ and the particle moves in the vacuum ($\varepsilon_1 = 1$). The dashed curve corresponds to the radiation in the vacuum ($\varepsilon_0 = \varepsilon_1 = 1$). For the heights of the peaks one has (from left to right) $(\hbar cT/q^2)dN_n/d\Omega \approx 2.8, 17, 16.9$. For $\rho_e \sim 1$ cm the corresponding radiation starts from centimeter wavelengths and falls into the terahertz region for higher harmonics. Note that for these wavelengths the imaginary part of the quartz permittivity is small.
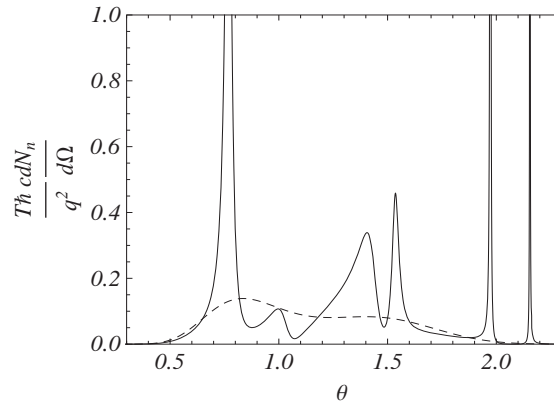
Figure 1. The dependence of the angular density for the number of radiated quanta, $(T\hbar c/q^2)dN_m/d\Omega$, per period T of the transverse motion, as a function of the angle θ for $\beta_{1\perp} = 0.9$, $\beta_{1\parallel} = 0.4$, $\rho_c/\rho_e = 0.95$, $n = 10$. The full curve corresponds to the radiation in the presence of a cylinder made of fused quartz ($\varepsilon_0 = 3.75$, $\varepsilon_1 = 1$) and the dashed curve is for the radiation in the vacuum ($\varepsilon_0 = \varepsilon_1 = 1$).

Analytical estimates for the heights and the widths of the peaks are given in [22]. These estimates show that at the peaks the angular density of the radiation intensity increases with increasing n. In realistic situations the growth of the radiation intensity is limited by several factors. In particular, the factors which limit the increase, are the imaginary part and the dispersion of the dielectric permittivity ε_1 (see the discussion in [22]). As it can be seen from (14), for a fixed value of the charge energy and in the case of circular motion, the product $\rho_e^2 dI_n/d\Omega$, with $n \neq 0$, is a function of the ratio ρ_c/ρ_e alone. From here it follows that for a fixed value of $\rho_e - \rho_c$ and for large values of ρ_c, the angular density of the radiation intensity, $dI_n/d\Omega$, decays as $1/\rho_e^2$. In this limit, the Cherenkov radiation remains only if the condition $\beta_{1\parallel} > 1$ is obeyed. The features of this radiation are discussed in [22]. Note that, in the exterior region the Cherenkov radiation is absent for the example presented in figure 1.

For general transverse motion of the charge and for a given radiation harmonic n, the angular density of the radiation intensity contains the summation over m (see (14)). Now for a given harmonic n we can have a set of peaks corresponding to different values of m and determined by the condition (17) replacing n in the indices of the cylinder functions by m. From the asymptotic formulas for the cylinder functions for large values of the order it follows that the peaks come from the part of the trajectory for which $|\lambda_1|\rho_e(t) < |m|$. At the peaks the coefficients $D_{m,n}^{(p)}$ in

the expression for the radiation intensity are estimated by $D_{m,n}^{(p)} \sim Y_{m,m,z}(n, \lambda_1), Y_{m+l,m}(n, \lambda_1)$, where the functions $Y_{m,m,z}(n, \lambda_1)$ and $Y_{m+l,m}(n, \lambda_1)$ are defined by the relations (5) and (16) taking in the integrand of (5) $F_m(\lambda_1 \rho_e(t)) = Y_m(\lambda_1 \rho_e(t))$. For large values of $m > 0$ we can use the Debye's asymptotic formula

$$Y_m(my) \sim \frac{2 (\operatorname{sgn} y)^{m+1} e^{m\zeta(y)}}{\sqrt{2\pi m}(1 - y^2)^{1/4}}, \quad |y| < 1, \tag{20}$$

with $\zeta(y) = \ln[(1 + \sqrt{1 - y^2})/|y|] - \sqrt{1 - y^2}$. The most strong peaks correspond to the part of the trajectory for which the function $\zeta(\lambda_1 \rho_e(t)/m)$ is maximum. For given values of n and m this corresponds to the minimum of the function $\rho_e(t)$. The parameters of the peaks depend on the form of the trajectory.

4. Conclusion

In the present paper we have considered the radiation from a charged particle moving around a dielectric cylinder along a helical trajectory the projection of which on the plane perpendicular to the cylinder axis is an arbitrary closed curve. Our aim was to study the sensitivity of the peaks appearing in the angular distribution of the radiation intensity with respect to distortions of the particle trajectory. By using the Green function from [10], the expression for the corresponding vector potential is presented in the region outside the cylinder.

We have derived a formula for the spectral-angular density of the radiation intensity in the exterior medium. The latter is given by the expression (14) with the coefficients defined by (15). In the case of a circular motion concentric with the cylinder axis, in (14) the term with $m = n$ survives only and we obtain the results previously discussed in [22]. Instead of a single peak in the angular distribution of the radiation intensity at a given harmonic n, for the case of general motion we have set of peaks corresponding to different values of m. The parameters of the peaks depend on the form of the trajectory. The most strong peaks correspond to the radiation from the part of the trajectory closest to the cylinder surface.

References

[1] Sokolov A A and Ternov I M 1986 *Radiation from Relativistic Electrons* (New York: ATP)
[2] Bordovitsyn V A (editor) 1999 *Synchrotron Radiation Theory and Its Development* (Singapore: World Scientific)
[3] Hofman A 2004 *The Physics of Synchrotron Radiation* (Cambridge: Cambridge University Press)
[4] Tsytovich V N 1951 Westnik MGU **11** 27
[5] Kitao K 1960 Progr. Theor. Phys. **23** 759
[6] Erber T White D and Latal H G 1976 Acta Phys. Austriaca **45** 29
[7] Schwinger J Tsai W-Y and Erber T 1976 Ann. Phys. **96** 303
[8] Erber T White D Tsai W-Y and Latal H G 1976 Ann. Phys. **102** 405
[9] Rynne T M Baumgartner G B and Erber T 1987 J. Appl. Phys. **49** 2233
[10] Grigoryan L Sh Kotanjyan A S and A.A. Saharian 1995 Sov. J. Contemp. Phys. **30** 1
[11] Kotanjyan A S Khachatryan H F Petrosyan A V and Saharian A A 2000 Sov. J. Contemp. Phys. **35** 1
[12] Kotanjyan A S and Saharian A A 2001 Sov. J. Contemp. Phys. **36** 7
[13] Kotanjyan A S and Saharian A A 2002 J. Contemp. Phys. **37** 263
[14] Kotanjyan A S and Saharian A A 2002 Mod. Phys. Lett. A **17** 1323
[15] Kotanjyan A S 2003 Nucl. Instrum. Methods **B201** 3
[16] Saharian A A and Kotanjyan A S 2005 J. Phys. A **38** 4275
[17] Saharian A A and Kotanjyan A S 2012 Int. J. Mod. Phys. B **26** 1250033
[18] Kotanjyan A S and Saharian A A 2012 J. Phys.: Conf. Ser. **357** 012009
[19] Saharian A A and Kotanjyan A S and Grigoryan M L 2007 J. Phys. A **40** 1405
[20] Saharian A A and Kotanjyan A S 2007 J. Phys. A **40** 10641
[21] Arzumanyan S R Grigoryan L Sh Khachatryan H F Kotanjyan A S and Saharian A A 2008 Nucl. Instrum. Methods **B266** 3703
[22] Saharian A A and Kotanjyan A S 2009 J. Phys. A **42** 135402